Article

Journal of
Biomedical Nanotechnology
Vol. 15, 979–992, 2019
www.aspbs.com/jbn

Peptide Self-Assembly Nanoparticles Loaded with Panobinostat to Activate Latent Human Immunodeficiency Virus

Qiyuan Kuai[1,†], Yu Wang[1,†], Fenghua Gao[1], Yingqiu Qi[2,3], Rui Wang[4], Yanbing Wang[1,5], Xiaofan Lu[4], Ying Zhao[2,6], Guangjun Nie[2,6], Min He[1], Hong Zhou[1], Xingwei Jiang[1,*], Suping Ren[1,7,*], and Qun Yu[1,7,*]

[1] *Beijing Institute of Transfusion Medicine, Beijing 100850, China*
[2] *CAS Key Laboratory for Biomedical Effects of Nanomaterials and Nanosafety, CAS Center for Excellence in Nanoscience, National Center for Nanoscience and Technology, Beijing 100190, China*
[3] *School of Basic Medical Sciences, Zhengzhou University, Henan 450001, China*
[4] *Beijing Key Lab for HIV/AIDS Research, Beijing Youan Hospital, Capital Medical University, Beijing 100069, China*
[5] *School of Life Sciences, Jilin University, Changchun 130012, China*
[6] *University of Chinese Academy of Sciences, Beijing 100049, China*
[7] *Beijing Advanced Innovation Center for Big Data-Based Precision Medicine, Beihang University, Beijing 100083, China*

Highly active antiretroviral therapy (HAART) can turn human immunodeficiency virus-1 (HIV-1) infection into a controllable chronic disease, but because of the presence of an HIV reservoir, it cannot completely eliminate the virus in HIV-infected patients. The activation of latent reservoirs is the key to the successful treatment of acquired immune deficiency syndrome (AIDS). As a class of latency-reversing agents (LRAs), histone deacetylase inhibitors (HDACis), such as panobinostat, have been the most widely investigated, but most of them have resulted in only a modest and transient activation of HIV latency. To improve the potency of latency activation, an injectable peptide self-assembly nanoparticle loaded with panobinostat (PNP-P) was designed with the ability to efficiently penetrate the cell to achieve better drug delivery and activation of latent HIV. The results confirmed that these nanoparticles could activate latently infected cells *in vitro* and *in vivo* and activate peripheral blood mononuclear cells (PBMCs) from latently infected patients *ex vivo*. Increased cellular drug uptake made the PNP-P more effective than panobinostat alone. Therefore, this strategy demonstrates that nanotechnology can help improve the activation of latent HIV, and this study lays a foundation for further development of LRA delivery systems for use against an HIV reservoir.

KEYWORDS: *HIV Reservoir, Latent HIV, Histone Deacetylase Inhibitors, Panobinostat, Peptide Self-Assembly, Nanoparticles.*

INTRODUCTION

Highly active antiretroviral therapy (HAART) can powerfully extend the life expectancy and improve the quality of life by achieving undetectable plasma viral RNA and the normalization of $CD4^+$ T cell levels in a majority of HIV-infected patients.[1] However, several studies have shown that human immunodeficiency virus (HIV) remains incurable owing to the HIV reservoir.[2–5] The reservoir is composed of a persistence of latently infected cells, including resting memory $CD4^+$ T cells and other cells belonging to the monocyte/macrophage lineage, that contain integrated transcription-silencing proviruses within their genome.[6–8] To eliminate these latently infected cells using activation of transcription, an ideal latency-reversing agent (LRA) must be active within the long-lived resting $CD4^+$ T cells. In addition, LRA needs to activate transcription from proviruses integrated into a multiplicity of sites throughout the genome.[9–11] Histone deacetylase inhibitors (HDACis), one kind of LRA, can promote activation of transcription by inhibiting histone deacetylases (HDACs).[12] To date, several independent studies

*Authors to whom correspondence should be addressed.
Emails: 13910216274@163.com, rensp12@yahoo.com, yuqun1970@outlook.com
†These two authors contributed equally to this work.
Received: 7 January 2019
Accepted: 8 February 2019

have demonstrated that HDACis can activate latent HIV-1 *in vitro* and *in vivo*.[9, 13–21]

Panobinostat is a highly potent hydroxamic acid panhistone deacetylase inhibitor that has been in clinical development for the treatment of multiple myeloma.[22] As the most promising LRA of activation of the HIV reservoir, previous studies have shown that panobinostat was able to induce HIV expression in latently infected cell line models, such as U1/HIV and ACH2, in primary $CD4^+$ T cell models of latency, and in resting $CD4^+$ T cells isolated from chronically infected HAART-suppressed patients.[23–25] Although panobinostat is in a leading position in the field of latent reservoir reactivation, some problems still exist. Panobinostat and some other LRAs are highly hydrophobic and have low solubility, resulting in low cellular uptake.[26] Panobinastat can only be used for oral administration, and there are problems of overdosing and low activation in *in vivo* applications.[27] As a result, the *in vivo* therapeutic effect is not satisfactory for clinic trails. Although the *in vivo* administration of panobinostat resulted in a modest (3.5-fold) increase of cell-associated HIV RNA in the peripheral blood, it did not reduce the number of latently infected cells in the panobinostat-treated patients.[28] Therefore, a way to improve the therapeutic effect of panobinostat is urgently needed.

A promising opportunity to improve latency activation is the development of enhanced delivery vehicles for existing molecules.[29–31] Several nanomedicines have been approved by the FDA and in other countries.[32] The advantages of nanoparticle delivery systems over many traditional drug delivery methods have been demonstrated in cancer therapy.[33–35] In this study, a treatment strategy is proposed that uses nanotechnology to activate latent HIV (Scheme 1). The nanoparticles enter the cell by endocytosis, releasing panobinostat, which would enhance the cellular uptake of panobinostat into HIV latently infected cells. The released panobinostat would enter the nucleus and act on HDACs to promote the transcription of latent HIV genes. The newly produced HIV could be killed by HARRT to achieve the goal of completely eliminating HIV. Based on the above treatment strategy, a novel cell-penetrating peptide (CPP) based amphiphilic peptide (cholesterol-KG2R9) monomer is designed and synthesized that self-assembles in the presence of chemotherapeutic drugs, such as panobinostat, to form stable nanoparticles. This process promotes cell activation to produce viruses by inhibiting HDACs. Given its ease of preparation, injectability, and cell penetration, this strategy is shown to be effective to improve small molecule drug delivery for the treatment of the HIV reservoir.

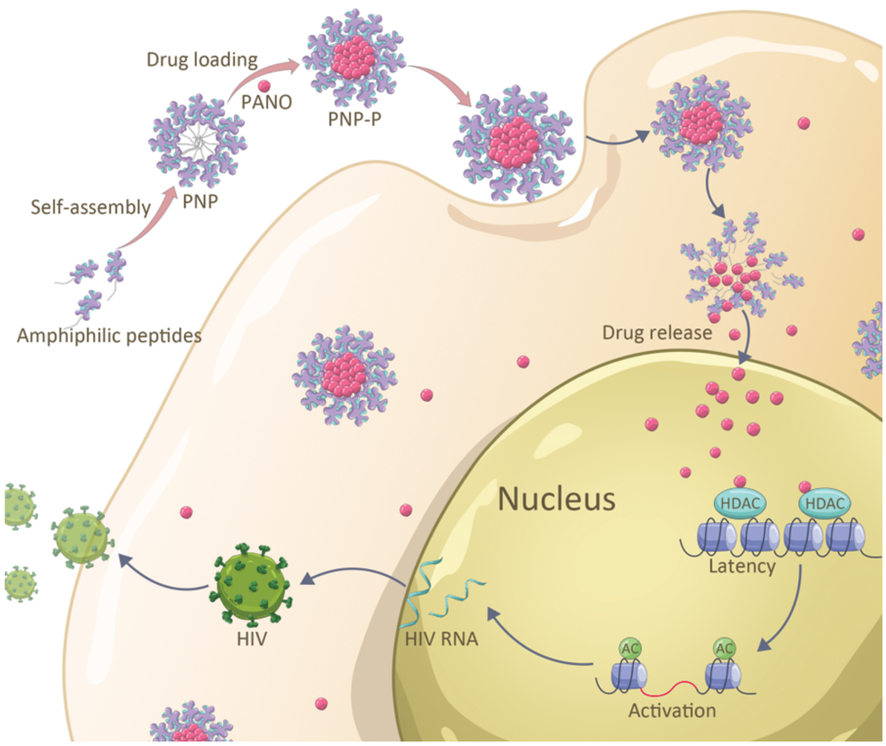

Scheme 1. **Schematic illustration of the composition, mechanism of activation of PNP-P. The nanoparticle formation process involves peptide self-assembling and drug loading. Nanoparticles penetrate into the cell, releasing drugs to activate latent HIV.**

EXPERIMENTAL REAGENTS AND INSTRUMENTS

Construction of the Peptide Nanoparticles

Cholesterol-KG2R9 peptide was synthesized by the Zhejiang Ontores Biotechnologies Co., Ltd. (Hangzhou, Zhejiang, China). Panobinostat (PANO) was purchased from Selleck Chemicals (Houston, TX, USA). Based on peptide self-assembly, PANO-free peptide nanoparticles (PNP) and PANO-loaded peptide nanoparticles (PNP-P) were prepared. Briefly, the peptide and panobinostat solutions were prepared by dissolving the powder at a concentration of 100 mg/mL in dimethylsulfoxide (DMSO). To prepare the PNP, 10 μL peptide solutions (1 mg cholesterol-KG2R9 peptide) were added to 1 mL of distilled water and sonicated for 10 minutes. For construction of the PNP-P, the cholesterol-KG2R9 peptide solutions (1 mg) and panobinostat solutions (0.5 mg) were mixed together. The mixed solutions were added to 1 mL of distilled water and sonicated for 10 minutes. After standing for one hour at room temperature, the aqueous phase was collected after centrifugation at 6000 rpm for 5 minutes.

Encapsulation Efficiency

The lyophilized PANO-loaded nanoparticles were dissolved in DMSO, and their concentration was measured using high-performance liquid chromatography (HPLC) (Agilent 1200, Santa Clara, CA, USA). The encapsulation efficiency (EE) was calculated according to the following formula: EE (%) = (mass of panobinostat encapsulated in nanoparticles/mass of panobinostat added) × 100%.

Characterization of the Nanoparticles

The morphology and particle size distribution of the PNP and PNP-P were characterized by transmission electron microscopy (TEM) (JEM-2100, JEOL Ltd., Tokyo, Japan) using a negative staining method with phosphotungstic acid (Zhongjingkeyi Technology, Beijing, China). Their zeta potentials were measured using dynamic light scattering (DLS) (Zetasizer Nano ZS90, Malvern, UK). The *in vitro* drug release profiles from the PNP-P were measured using the dialysis method. Briefly, aliquots of nanoparticles solution were injected into dialysis cartridges with a molecular weight cutoff value of 1 kDa. The cartridges were dialyzed against 40 mL of phosphate buffer saline (PBS) with 10% fetal bovine serum (FBS) and shaken at 37 °C at 100 rpm. The concentrations of panobinostat that remained in the dialysis cartridge at different time points were measured using HPLC (Agilent 1200).

Stability Evaluation of the Nanoparticles

The 3,3′-dioctadecyloxacarbocyanine perchlorate (Dio) (Invitrogen, Carlsbad, CA, USA) was added into the assembled PNP solutions with an ultrasonicator (KQ2200E, Kunshan, Jiangsu, China) operated at 100 W for 10 minutes. A fluorescence spectrophotometer (HITACHI F-4600, Japan) was used to measure the fluorescence intensity of the solution (excitation at 484 nm) at different time points.

The PNP-P was incubated with 10% FBS/PBS for 48 hours, and the morphologies of the resulting nanostructures were characterized by TEM using a negative staining method with phosphotungstic acid after incubation.

Cell Culture

J-Lat Tat-GFP Clone A72, ACH2, and U1/HIV cell lines were provided by the National Institute of Health AIDS Research and Reagent Program, Division of AIDS, NIAID, NIH. J-Lat Tat-GFP Clone A72 is an HIV latently infected Jurkat T-cell line that integrates a genome that latently expresses green fluorescence protein (GFP) under an HIV long terminal repeat (LTR).[36] The ACH2 cell line is an HIV-1 latent T cell line with one integrated proviral copy that is derived from CEM, a human T cell line. U1/HIV cells are subclones of U937 cells that are chronically infected with HIV-1 but show a minimal constitutive expression of the virus. Peripheral blood mononuclear cells (PBMCs) were isolated from human whole blood as previously described.[2]

All of the cells were cultured in RPMI1640 medium (Gibco, Grand Island, NY, USA) supplemented with 10% fetal bovine serum (FBS) (ExCell Bio, Shanghai, China) in an incubator at 37 °C with 5% CO_2.

Apoptosis Assay

To quantify the percentage (%) of apoptosis induction in drug-treated cells, the Annexin V Detection Kit APC (Invitrogen) assay was used. J-Lat Tat-GFP Clone A72, ACH2, and U1/HIV cells were seeded into 12-well plates (1×10^6 cells/well) and cultured with various drug formulations (final concentration 20 nM) for 4 hours. The drugs were removed using centrifugation, then the cells were cultured for 24 hours. The cells were collected using centrifugation and stained with Annexin V APC and a propidium iodide (PI) staining solution (Invitrogen) at room temperature in the dark. Next, the cells were analyzed immediately using flow cytometry (BD FACSAria, San Jose, CA, USA).

Cell Uptake Assay

ACH2 and U1/HIV cells were plated in 12-well plates (1×10^6 cells/well) and incubated with equal amounts of fluorescein isothiocyanate (FITC) (Sigma-Aldrich, St. Louis, MO, USA) and FITC-labeled PNP for 4 hours. The cells were observed under a confocal microscopy (Nikon Corp., Tokyo, Japan). The fluorescence intensities of the FITC-positive cells were then measured using a flow cytometer (BD FACSAria).

Analysis of Histone Acetylation

ACH2 and U1/HIV cells were seeded into 12-well plates (1×10^6 cells/well) and cultured with various drug formulations (final concentration 20 nM) for 4 hours. The drugs were removed by centrifugation, then the cells were cultured for 24 hours. Fixation and permeabilization of cells were performed using the eBioscience™ Foxp3/Transcription Factor Staining Buffer Set (Invitrogen). The cells were then washed and stained with anti-acetyl-histone H3 phycoerythrin (PE)-labeled antibody (Millipore, Temecula, CA, USA; catalog No. FCABS325PE), anti-acetyl-histone H4 PE-labeled antibody (Millipore; catalog No. FCABS326PE), or PE-labeled IgG antibody (Santa Cruz Biotechnology, Dallas, TX, USA; catalog No. sc-3745) for 30 minutes. They were washed twice and resuspended in a 2% paraformaldehyde solution (Solarbio, Beijing, China) for analysis using flow cytometry (BD FACSAria).

Cell Line Activation Assay

J-Lat Tat-GFP Clone A72 cells were seeded into 12-well plates (1×10^6 cells/well) and cultured with various drug formulations (final concentration 20 nM) for 4 hours. The drugs were removed using centrifugation, then the cells were cultured for 24 hours. The percentage of GFP-positive cells was then measured using a flow cytometer (BD FACSAria).

ACH2 and U1/HIV cells were seeded into 12-well plates (1×10^6 cells/well) and cultured with various drug formulations (final concentration 20 nM) for 4 hours. The drugs were removed using centrifugation, and then the cells were cultured for 24 hours. The cells were washed twice in PBS and stained with FITC anti-human CD69 antibody (BioLegend, San Diego, CA, USA; catalog No. 310904) or FITC mouse IgG1 antibody (BioLegend; catalog No. 400109) for 15 minutes at room temperature. The cells were washed twice and resuspended in a 2% paraformaldehyde solution (Solarbio) for flow cytometry analysis (BD FACSAria). For intracellular p24 detection, fixation and permeabilization of the cells were performed using the eBioscience™ Foxp3/Transcription Factor Staining Buffer Set (Invitrogen). The cells were then washed and stained with KC57-RD1 antibody (Beckman Coulter, Brea, CA, USA; catalog No. 6604665) or PE Mouse IgG1 antibody (BioLegend; catalog No. 400111) for 30 minutes, washed twice, and resuspended in a 2% paraformaldehyde solution (Solarbio) for flow cytometry analysis (BD FACSAria). The levels of HIV-1 p24 gag were determined using an ELISA assay as described by the manufacturer (R&D Systems, Minneapolis, MN, USA) for the detection of p24 in cell culture supernatants.

Quantification of Viral Outgrowth

ACH2 and U1/HIV cells were seeded into 12-well plates (1×10^6 cells/well) and cultured with various drug formulations (final concentration 20 nM) for 4 hours. The drugs were removed using centrifugation, then the cells were cultured for 24 hours. Two HIV-infected patients being treated with HAART for at least two years and with undetectable viral loads (less than 50 copies/mL) for more than six months and $CD4^+$ T cell levels above 300 cells/μL were recruited from the Beijing You-An Hospital, Beijing. Informed consent was obtained from all of the participants with the approval and oversight of the Beijing You-An Hospital Internal Review Board. PBMCs from the patient's blood were seeded into 12-well plates (1×10^6 cells/well) and cultured with various drug formulations (final concentration 20 nM) for 5 days. Cell culture supernatants were collected using centrifugation. HIV-1 copies in the culture supernatant were quantified using the Abbott RealTime HIV-1 Kit and the Abbott m2000 RealTime PCR System (Des Plaines, IL, USA).

Animal Studies

All of the animal experiments were reviewed and approved by the Institutional Animal Care and Use Committee of the Academy of Military Medical Science, Beijing, China (IACUC-DWZX-2018-017), and the animals were housed and handled in accordance with the guidelines of the National Institutes of Health. Female M-NSG (NOD-Prkdc^{scid}Il2rg^{em1}/Smoc) mice (8 weeks old, 20 g) were obtained from Shanghai Model Organisms (Shanghai, China). Experiments were performed after an acclimatization period of 7 days. Twenty-eight mice were intraperitoneally injected with J-Lat Tat-GFP Clone A72 cells (2×10^7 cells each) and randomly divided into four groups, with seven in each group. These groups consisted of a control group (saline, i.p.), a PNP group (i.p.), a PANO group (2.5 mg/kg, i.p.), and a PNP-P group (2.5 mg/kg, i.p.). After injection with various drug formulations for 24 hours, the anesthetized mice were killed. The J-Lat Tat-GFP Clone A72 cells were washed out with PBS from the mouse abdominal cavity. The red blood cells were removed using a red blood cell lysis buffer (Solarbio). The remaining cells were stained with APC anti-human CD3 antibody (BioLegend; catalog No. 344812) and APC Mouse IgG1 and κ Isotype Ctrl (FC) antibody (BioLegend; catalog No. 400121) for 15 minutes at room temperature. The percentage of GFP-positive cells was then measured using a flow cytometer (BD FACSAria).

Statistical Analysis

The results are expressed as means $\pm$ standard deviations (SD). The statistical analyses were performed using Prism 7 (San Diego, CA, USA). An ordinary two-way analysis of variance (ANOVA) test was used to determine whether there was an overall difference among the various drug formulations, and multiple comparisons were performed using Tukey's test. $p < 0.05$ was considered to be significant (*), and $p < 0.01$ was considered to be very significant (**).

RESULTS AND DISCUSSION

Characterization of the PNP-P

The nanoparticle drug delivery system designed in this study is based on the amphiphilic peptide (cholesterol-KG2R9). This peptide contains nine positively charged arginine (R) residues, two glycine (G) residues, one positively charged lysine (K), and cholesterol as a hydrophobic tail. The nine arginine (R9) residues have been verified to have superlative cell-penetrating efficiency among previously reported oligopolyarginines. These residues were engineered at the hydrophilic block of the CPP to provide cationic charges for effective membrane translocation.[37–39] Cholesterol is an important component of cell membranes and has been well documented to drive peptide self-assembly and improve membrane permeability.[40–42] The amphiphilic peptide-cholesterol monomer can be easily self-assembled to form a core–shell structure peptide nanoparticle (PNP) with a hydrophobic cholesterol core and a hydrophilic cationic R9 peptide shell facing the surrounding water environment. The hydrophobic drug, panobinostat, can be encapsulated by PNP to form panobinostat-loaded nanoparticles PNP-P (Scheme 1). The critical aggregation concentration of cholesterol-KG2R9 is 75 mg/L. After optimization, 1 mg/mL cholesterol-KG2R9 was used for the entire study. Initial analysis of the PNP and PNP-P morphologies using TEM revealed a spherical shape and a narrow size distribution, which is an excellent range for cell penetration

Table I. Encapsulation efficiency of PNP-P with different masses of panobinostat added.

Panobinostat added (mg)	0.075	0.1	0.25	0.5	0.75
Panobinostat encapsulated (mg)	0.0639	0.0844	0.2185	0.3646	0.4087
Encapsulation efficiency (%)	85.20	84.40	87.40	72.92	54.49
Drug loading ratio (%)	11.33	14.44	30.41	42.17	44.98

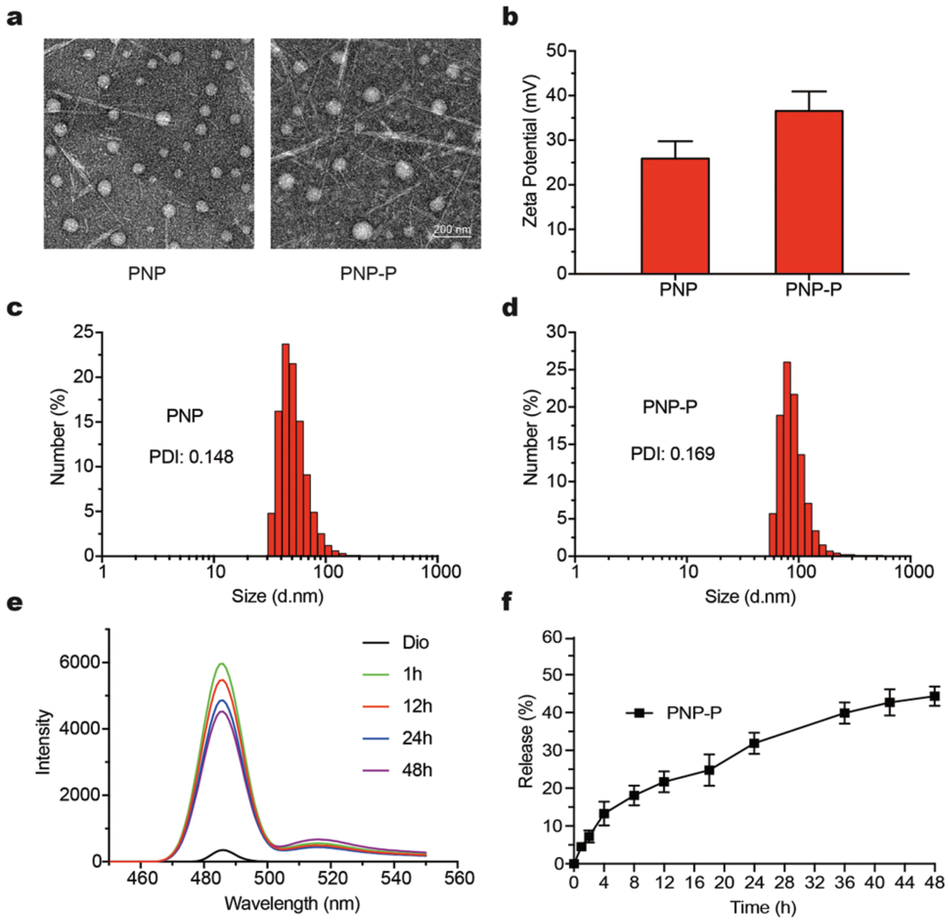

Figure 1. **Characterization of PNP-P. (a) TEM images of PNP and PNP-P. The scale bar is 200 nm. (b) Zeta potentials of PNP and PNP-P detected by DLS. Data are mean + SD ($n = 3$). Size of PNP (c) and PNP-P (d) found using dynamic light scattering (DLS). (e) The fluorescence intensity of Dio inserted in PNP after incubation with 10% FBS/PBS for different periods of time. (f) The drug release profiles of PNP-P in 10% FBS/PBS.**

and retention (Fig. 1(a)).[43] Due to the existence of the R9 residues, the nanoparticles showed a positive zeta potential (Fig. 1(b)). Also, during the drug loading process, the zeta potentials of the nanoparticles in the PBS (pH 7.4) increased from 25.9 ± 3.1 mV (PNP) to 36.5 ± 3.6 mV (PNP-P). The peptide-cholesterol formed spherical nanoparticles that had diameters of approximately 40 nm (Figs. 1(c and d)). When loaded with panobinostat, their diameters increased to approximately 80 nm. To optimize the drug-loading efficacy, different

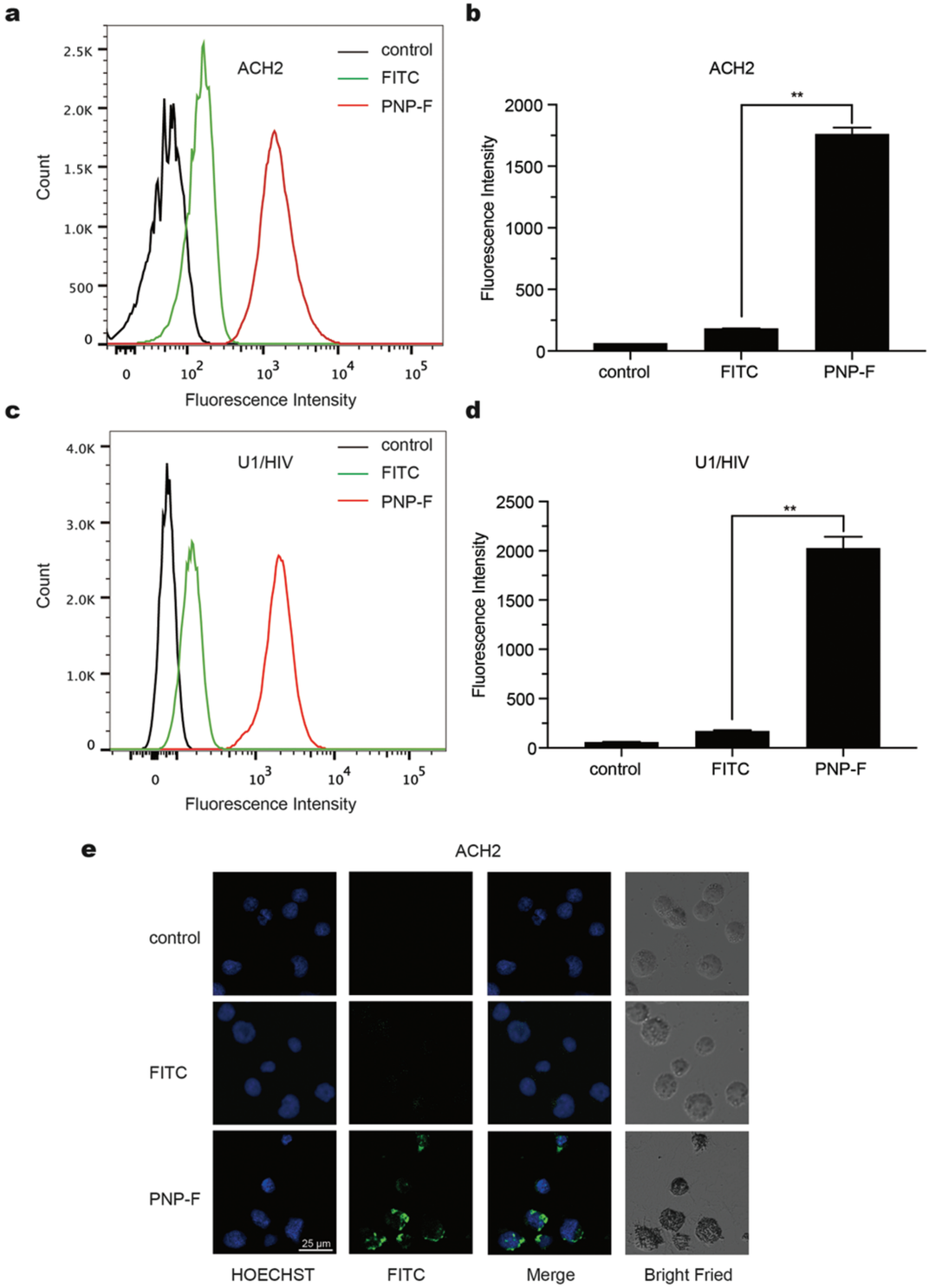

Figure 2. **Continued.**

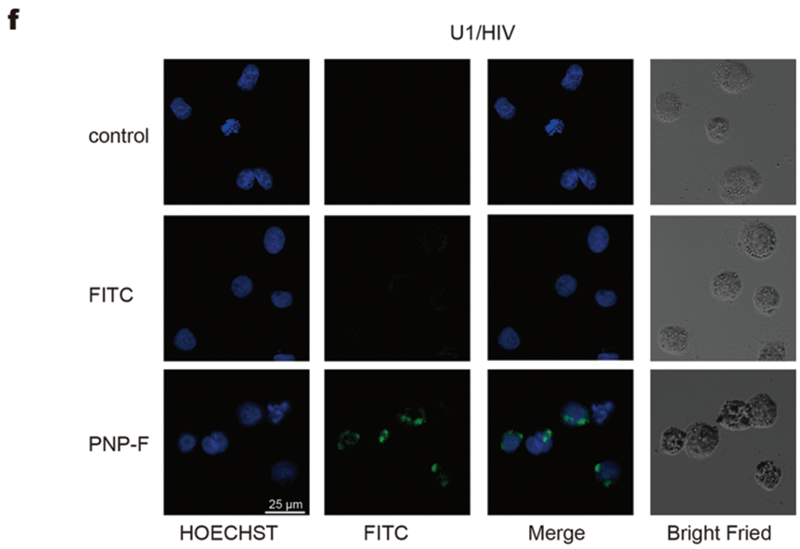

Figure 2. Quantitative analysis of cellular uptake in ACH2 and U1/HIV cells. (a) ACH2 cells were incubated with FITC for 4 hours and with FITC-labelled nanoparticles (PNP-F) for 4 hours. The control group consisted of untreated cells. Flow cytometry measurements of FITC signals in the ACH2 cells. (b) The fluorescence intensity of FITC in the ACH2 cells belonging to (a). Data are mean + SD ($p < 0.01$, $n = 3$). (c) U1/HIV cells were incubated with FITC for four hours and with PNP-F for 4 hours. The control group consisted of untreated cells. Flow cytometry measurements of FITC signals in the U1/HIV cells. (d) The fluorescence intensity of FITC in U1/HIV cells belonging to (c). Data are means + SD (**$p < 0.01$, $n = 3$). (e) Confocal images of ACH2 cells. Cells were incubated with FITC for 4 hours and with PNP-F for 4 hours. The control group consisted of untreated cells. Nuclei were stained with Hoechst (blue), and FITC signals were green. (f) Confocal images of U1/HIV cells. The cells were incubated with FITC for 4 hours and with PNP-F for 4 hours. The control group consisted of untreated cells. Nuclei were stained with Hoechst (blue), and FITC signals were green.**

PANO-to-peptide ratios were evaluated (Table I). Stable nanoparticles formed at panobinostat concentrations of up to 750 μg/mL, suggesting a high PANO-loading capacity for the peptide nanoparticles. To detect the stability of the designed nanoparticles, 3,3′-dioctadecyloxacarbocyanine perchlorate (Dio, a dye that can only be activated when embedded in micelles, the membrane lipid bilayer, or liposomes) was encapsulated in the hydrophobic core of the PNP. After incubation with a 10% fetal bovine serum (FBS) in PBS for 48 hours, the fluorescence intensity remained at 80%, demonstrating the integrity of the PNP micelle structure (Fig. 1(e)). *In vitro* drug release profiles were studied in 10% FBS/PBS at a pH of 7.4. As shown in Figure 1(f), approximately 45% of the panobinostat was released from the nanoparticle after 48 hours *in vitro*. These data suggested that there was a sustained release of panobinostat over time that paralleled the stability of PNP-P. The above results demonstrated the successful construction of PNP-P, which exhibited a uniform nanostructure with suitable size and surface charges, favorable stability, as well as controlled drug release. With these traits, PNP-P would increase *in vitro* and *in vivo* therapeutic efficacy.

Nanoparticle Increased Cellular Uptake

To quantitatively evaluate PNP as delivery vehicles for target cells, they were loaded with the fluorescent dye, FITC, and incubated with ACH2 and U1/HIV cells for four hours. The uptake was then evaluated using flow cytometry (Figs. 2(a–d)). The fluorescence intensity of the PNP-F group was much higher than the free FITC group in both of the cell lines. The PNP-F exhibited a higher efficiency to enter both cell types than the free FITC group, demonstrating that the cell penetration mediated by the CPP and cholesterol-based nanoparticles was an efficient strategy for drug delivery into cells. The same phenomenon was also seen in the laser confocal microscopy analysis (Figs. 2(e and f)). In contrast, the free FITC group showed little uptake during the same incubation period. The merged images show cytosolic and nuclear localization of the PNP-F. Some green fluorescence was distinct from the nuclear Hoechst stain, and some overlapped with the nuclear area. It is likely that PNP loaded with drugs, including panobinostat, would show a similar trafficking pattern and release their cargo in both the cytoplasm and the nuclear area, thereby reducing non-specific distribution before the drugs enter the cells, thus increasing the intracellular concentration of the drugs. This effect would, in turn, enhance drug interactions with HIV components and improve their therapeutic effects.

PNP-P Displayed Low Cytotoxicity and Increased Histone Acetylation Levels in Latently Infected Cell Lines

Since the cell transport efficiency of panobinostat was improved by using PNP, the cytotoxicity of various

panobinostat formulations on the viability of J-Lat Tat-GFP Clone A72, ACH2, and U1/HIV cells were measured. To measure cytotoxicity, the three cell lines (Fig. 3(a)) were treated with various drug formulations (final concentration 20 nM) and analyzed using flow cytometry for the apoptotic/necrotic markers, Annexin V, and PI. Based on a quadrant analysis, PNP and PNP-P (each compared to control and free panobinostat) negligibly increased early apoptosis (Annexin V + PI-cells) and late apoptosis/necrosis (Annexin V + PI + cells) in all of the cells. The results demonstrated that the proposed nanoparticle delivery system was not cytotoxic, but did increase drug delivery efficiency. Apoptosis modestly increased after treatment with free panobinostat and PNP-P compared to the control group and PNP, but approximately 90% of the cells did not lose viability (Figs. 3(b–d)). The same drug concentration (20 nM) was also chosen by other groups for *in vitro* assays, which is consistent with our optimization results.[27,44] Therefore, the concentration (20 nM) and time (4 hours) of administration was suitable for the following assays.

Most of the evidence has shown that the regulation of histone acetylation on the HIV promotor is critical for promoting the expression of HIV.[45,46] HDACis can induce hyperacetylation of the HIV promoter-associated nucleosomes to activate latent HIV by suppressing cellular HDAC expression and binding to the HIV promoter.[47] To measure the histone acetylation, ACH2 and U1/HIV cells were treated with various drug formulations (final concentration 20 nM) and analyzed using flow cytometry for

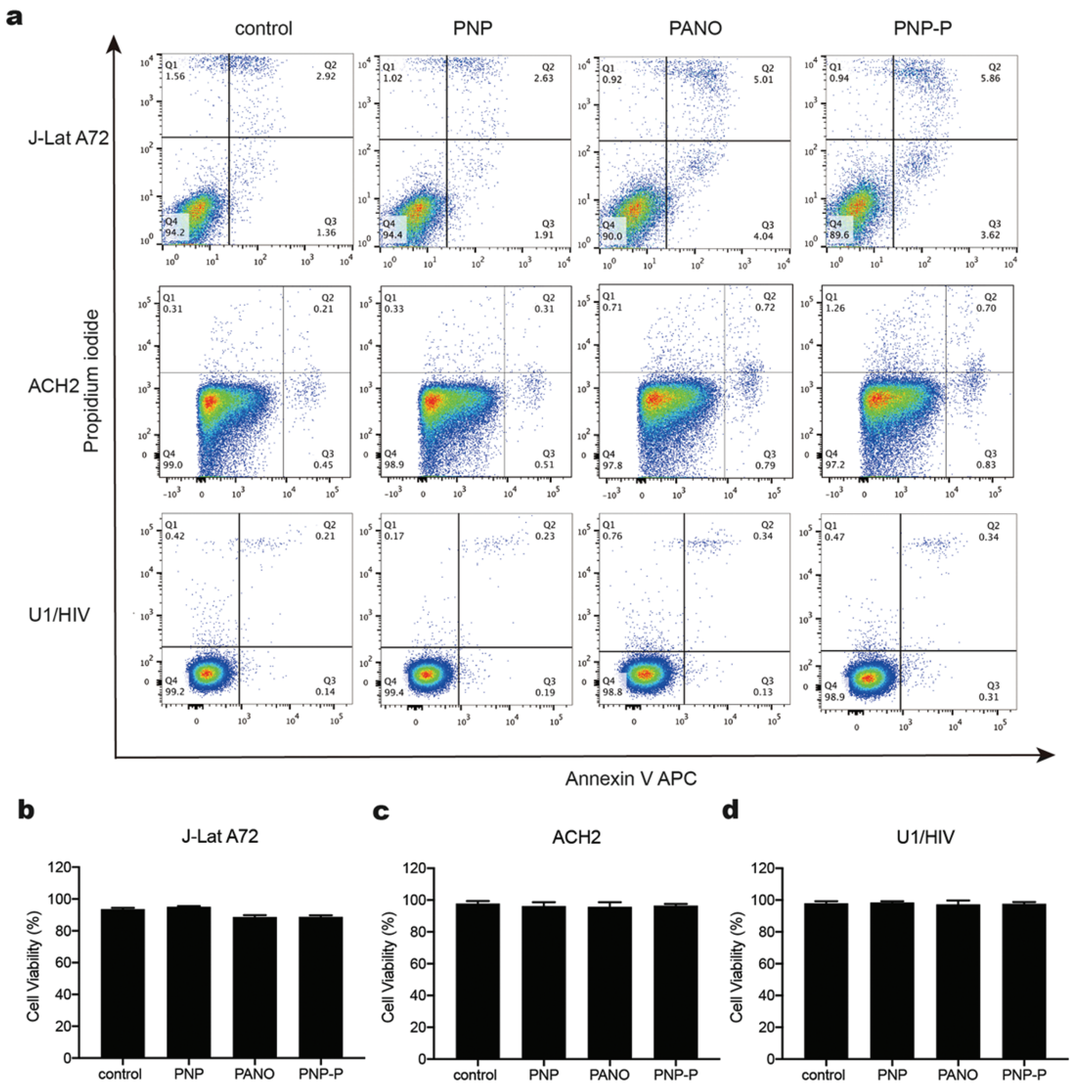

Figure 3. **Effects of PANO-loaded nanoparticles on cytotoxicity in ACH2 and U1/HIV cells. (a) J-Lat Tat-GFP Clone A72, ACH2, and U1/HIV cells were cultured with various drug formulations (final concentration 20 nM). Apoptosis was assessed using flow cytometry. The percentages of J-Lat Tat-GFP Clone A72 (b), ACH2 (c), and U1/HIV (d) cells as detected by flow cytometry belonging to (a). Data are mean + SD ($n = 3$).**

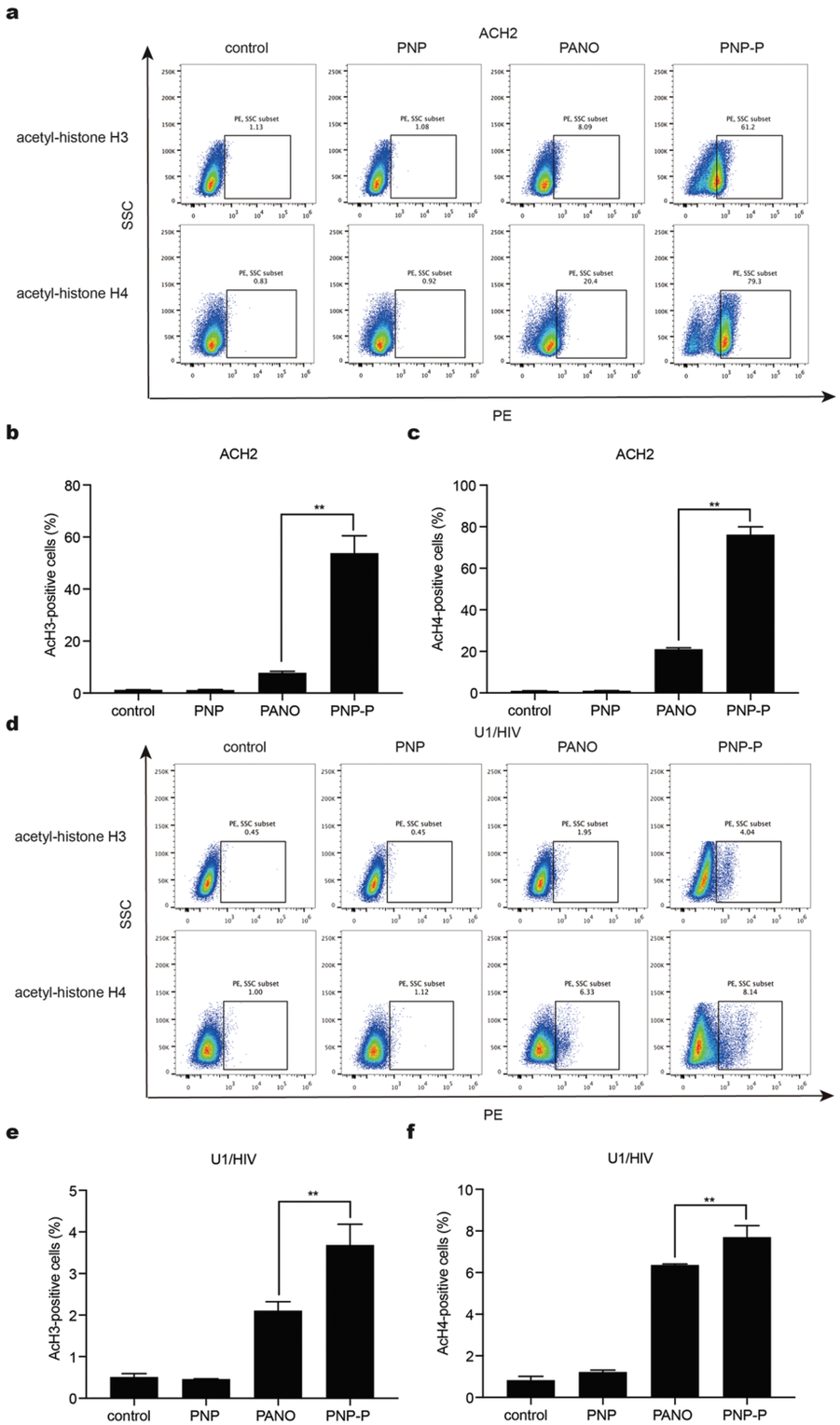

Figure 4. **Effects of PANO-loaded nanoparticles on histone acetylation in ACH2 and U1/HIV cells. (a) ACH2 cells were incubated with various drug formulations (final concentration of 20 nM). Histone H3 and histone H4 acetylation were measured using flow cytometry. The percentages of acetyl-Histone H3-positive (b) and acetyl-Histone H4-positive (c) ACH2 cells as detected by flow cytometry belonging to (a). Data are mean + SD (** $p < 0.01$, $n = 3$). (d) U1/HIV cells were incubated with various drug formulations (final concentration of 20 nM). Histone H3 and histone H4 acetylation were measured using flow cytometry. The percentages of acetyl-Histone H3-positive (e) and acetyl-Histone H4-positive (f) U1/HIV cells as detected by flow cytometry belonging to (d). Data are mean + SD (** $p < 0.01$, $n = 3$).**

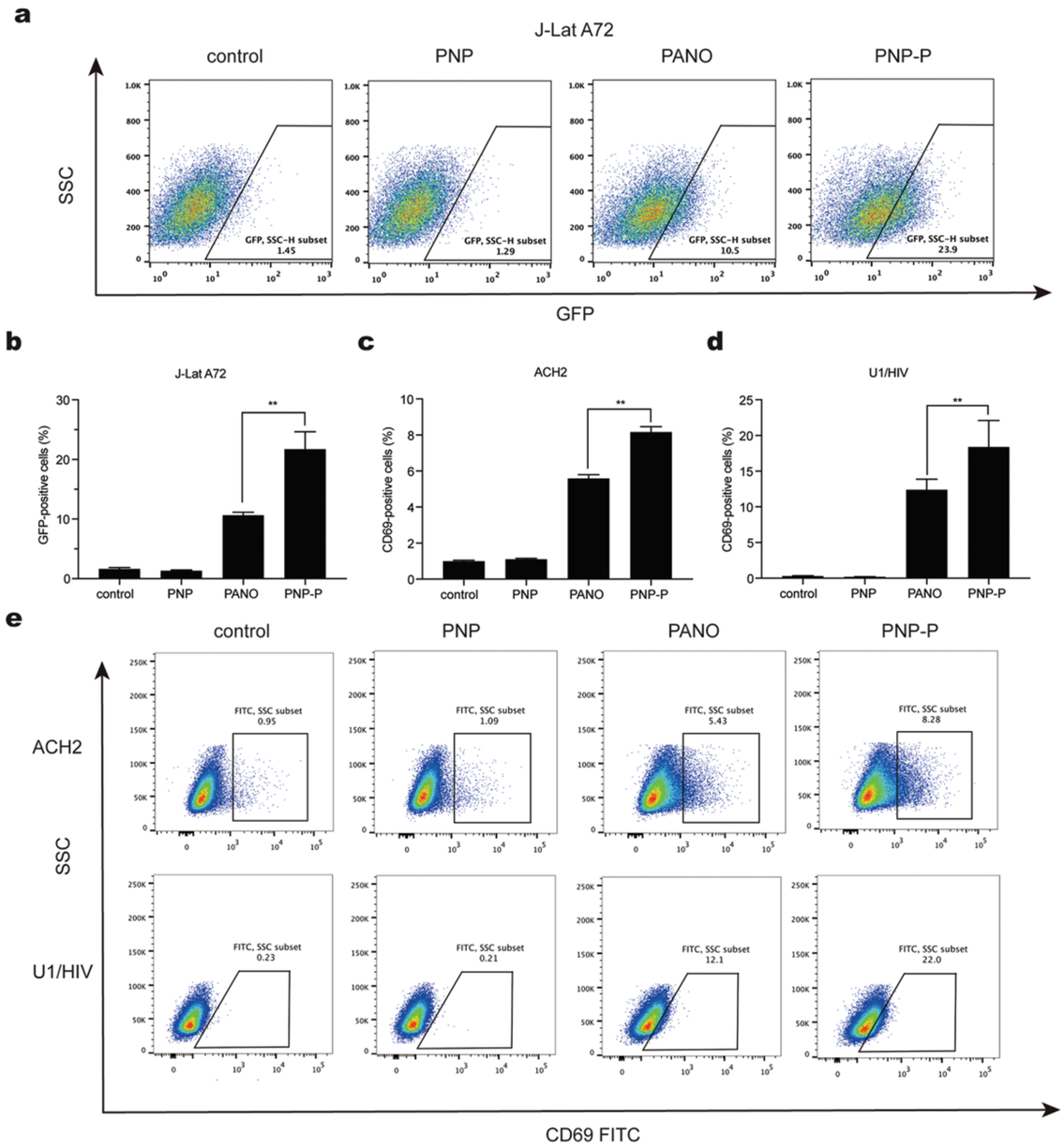

Figure 5. Activation efficacy of PANO-loaded nanoparticles in latently infected cell lines. (a) J-Lat Tat-GFP Clone A72 cells were treated with various drug formulations (final concentration of 20 nM). The GFP-positive cells were measured using flow cytometry. (b) GFP expression of J-Lat Tat-GFP Clone A72 cells treated with various drug formulations belonging to (a). Data are mean + SD ($p < 0.01$, $n = 3$). ACH2 (c) and U1/HIV (d) cells were treated with various drug formulations (final concentration of 20 nM). Expression of the activation marker, CD69, was measured using flow cytometry. Data are mean + SD (** $p < 0.01$, $n = 3$). (e) Representative flow cytometry plots of CD69 expression in ACH2 and U1/HIV cells treated with various drug formulations.**

histone H3 and histone H4 acetylation. Compared to free panobinostat, histone H3 and histone H4 acetylation levels of the PNP-P treated group were significantly enhanced in both cells (Fig. 4). In the ACH2 cells, the histone H3 acetylation level was dramatically upregulated from 1.13% to 61.2%, and acetylated histone H4 was upregulated from 0.83% to 79.3% (Fig. 4(a)). In contrast, the histone H3 and histone H4 acetylation levels of U1/HIV were upregulated modestly, but still statistically significant (Figs. 4(e and f)). These results demonstrated that the designed nanoparticle delivery system was able to improve the potency of panobinostat for the inhibition of HDACs, which is important for the activation of the HIV reservoir.

PNP-P Activated Latent HIV in Latently Infected Cell Lines and PBMCs from HIV-Infected Patients

To determine whether panobinostat-loaded nanoparticles are capable of stimulating HIV from latency, the J-Lat

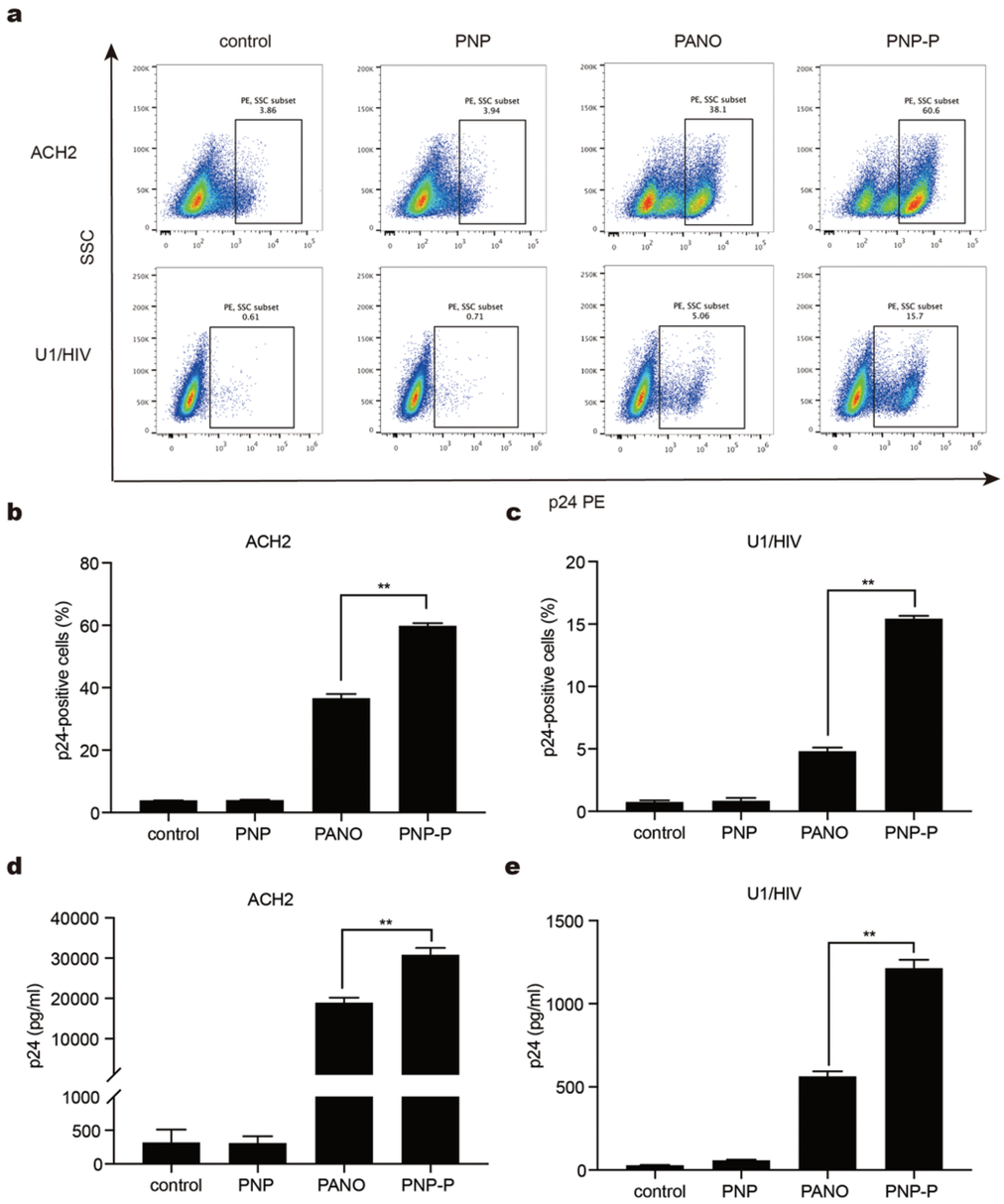

Figure 6. P24 expression in ACH2 and U1/HIV cells treated with PANO-loaded nanoparticles. ACH2 and U1/HIV cells were treated with various drug formulations (final concentration of 20 nM). (a) The expression of intracellular p24 was measured using flow cytometry. The percentages of intracellular p24-positive ACH2 (b) and U1/HIV (c) cells as detected by flow cytometry belonging to (a). Data are mean + SD ($p < 0.01$, $n = 3$). The p24 levels in the supernatant of ACH2 (d) and U1/HIV (e) cells were detected using ELISA. Data are mean + SD (**$p < 0.01$, $n = 3$).**

Tat-GFP cell line models were utilized. These models express GFP upon activation of latent HIV.[36] J-Lat Tat-GFP Clone A72 cells were treated with various drug formulations (final concentration of 20 nM) and analyzed using flow cytometry for the expression of GFP. Compared to free panobinostat, the expression of GFP in PNP-P-treated cells was significantly enhanced (Figs. 5(a and b)). Increased GFP expression suggested that the proposed strategy could play a role in the activation of the HIV reservoir.

ACH2 and U1/HIV are two HIV latently infected cell lines that harbor the full-length virus and secrete p24 (the structural protein of the HIV capsid) to the medium when the virus is activated. To assess the effect of PNP-P on the activation of ACH2 and U1 cells, the expression of CD69, p24, and viral copies were detected using flow cytometry, ELISA, and real-time PCR. CD69 was the first to be detected, and this is an early activation marker that is expressed in T cells. After incubation with various drug formulations, PNP-P induced more expression of CD69

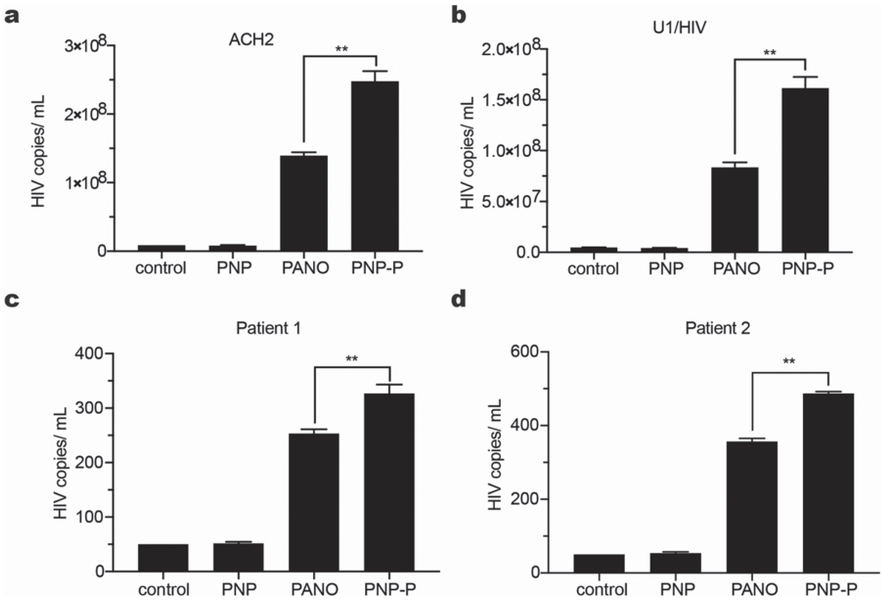

Figure 7. Effects of PANO-loaded nanoparticles on viral outgrowth in latently infected cell lines and patients' PBMCs. ACH2 (a), U1/HIV (b) cells, and PBMCs (c, d) from two latently infected patients were treated with various drug formulations (final concentration of 20 nM). HIV-1 copies in the culture supernatant were quantified using the Abbott RealTime HIV-1 Kit and the Abbott m2000 RealTime PCR System. Data are mean + SD ($p < 0.01$, $n = 3$).**

in both of the cell lines compared with free panobinostat (Figs. 5(c–e)). Similar results appeared for the expression of p24. The expression of intracellular p24 was significantly increased by treatment with PNP-P (Figs. 6(a–c)). Compared to free panobinostat, PNP-P also increased the median p24 levels in the ACH2 and U1 cell supernatants by 1.63-fold and 2.16-fold, respectively (Figs. 6(d and e)). In addition, viral copies progressively increased, reaching about 1.8-fold higher levels than with free panobinostat after 4 hours of incubation with PNP-P (Figs. 7(a and b)). These results demonstrate that PNP-P could induce the expression of latent HIV, and it was more effective than the free drug at activating latent HIV in cell lines.

To verify the results obtained in the latently infected cell lines, PBMCs were isolated from two latently infected patients under at least two years of HAART with undetectable viral loads for at least six months. After isolation, the PBMCs were treated with various drug formulations (final concentration of 20 nM) for 5 days. The ability of PNP-P to induce viral production was tested. PNP-P induced more viral production than free panobinostat (Figs. 7(c and d)). These results indicated that the designed

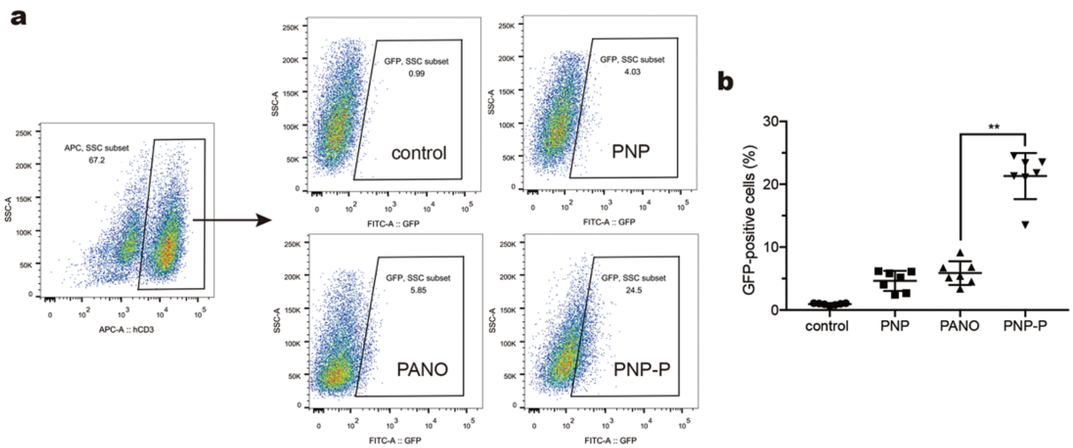

Figure 8. PNP-P activated J-Lat Tat-GFP Clone A72 cells *in vivo*. (a) M-NSG mice were injected with J-Lat Tat-GFP Clone A72 cells. Representative flow cytometry plots of human CD3$^+$ cells analyzed for the induction of the GPF expression after incubation with various drug formulations for 24 hours *in vivo*. (b) GFP expression of human CD3$^+$ cells belonging to (a). Data are mean ± SD ($p < 0.01$, $n = 7$).**

nanosystem could not only improve the efficacy in the cell lines, but also in the primary cells. The effect in the primary cells further confirmed the activation of latent HIV by PNP-P. The increased activation ability of *ex vivo* samples made this peptide nanoparticle delivery system more clinically applicable.

PNP-P Activated J-Lat Tat-GFP Clone A72 Cells *In Vivo*

Encouraged by the noticeable *in vitro* HIV reservoir activation efficacy, the effect of PNP-P on activation of latent HIV in mice was investigated. J-Lat Tat-GFP Clone A72 cells were injected into the abdominal cavity of M-NSG mice (severe immunodeficient mice). After treatment with various drug formulations for one day, all of the mice survived normally, and the injected cells were extracted for flow detection. J-Lat Tat-GFP Clone A72 cells injected into the mice were selected for analysis of GFP expression using anti-human CD3 antibody (Fig. 8(a)). The free drug group showed only a small activation effect *in vivo*, similar to the PNP group. Compared with the free drug group, PNP-P showed an increased effect of latent HIV activation (Fig. 8(b)). These results indicated that the proposed drug delivery system could help improve the activation efficiency of LRAs *in vivo*. Due to the biocompatibility of the nanomaterials and the previous activation results of the patient's *ex vivo* samples, this strategy may be used to enhance HIV latency purging in future clinical trials.

CONCLUSIONS

In conclusion, to overcome deficiencies of LRAs in the activation of the HIV reservoir, such as poor solubility and activation efficiency, a nanoparticle delivery system based on peptide self-assembly, referred as to PNP-P, was successfully engineered. The designed nanomaterials had good biocompatibility and biodegradability with enhanced cell penetration capacity, showing their ability to be injected. Due to increased cellular uptake, PNP-P achieved a high activation efficacy against latent HIV both *in vivo* and *in vitro*. PNP-P also showed great potential for improvement of the LRA activation effect. This strategy lays the foundation for the further development of LRA delivery systems for use against an HIV reservoir.

Acknowledgments: This work was supported by the National Key R&D Program of China (2017YFSF110080), Program for the 13th Five-year Plan of China (2017ZX10202101004), the National Science and Technology Major Project of China (2018ZX09J18111), and Beijing key lab for HIV/AIDS research (BZ0089).

REFERENCES

1. O. O. Oguntibeju, Quality of life of people living with HIV and AIDS and antiretroviral therapy. *HIV AIDS (Auckl).* 4, 117 (**2012**).
2. Q. Kuai, X. Lu, Z. Qiao, R. Wang, Y. Wang, S. Ye, M. He, Y. Wang, T. Zhang, H. Wu, S. Ren, and Q. Yu, Histone deacetylase inhibitor chidamide promotes reactivation of latent human immunodeficiency virus by introducing histone acetylation. *J. Med. Virol.* 90, 1478 (**2018**).
3. C. T. Costiniuk and M. A. Jenabian, HIV reservoir dynamics in the face of highly active antiretroviral therapy. *AIDS Patient Care STDS* 29, 55 (**2015**).
4. T. W. Chun, S. Moir, and A. S. Fauci, HIV reservoirs as obstacles and opportunities for an HIV cure. *Nat. Immunol.* 16, 584 (**2015**).
5. G. H. Li, L. Henderson, and A. Nath, Astrocytes as an HIV reservoir: Mechanism of HIV infection. *Curr. HIV Res.* 14, 373 (**2016**).
6. A. Alexaki, Y. Liu, and B. Wigdahl, Cellular reservoirs of HIV-1 and their role in viral persistence. *Curr. HIV Res.* 6, 388 (**2008**).
7. C. Van Lint, S. Bouchat, and A. Marcello, HIV-1 transcription and latency: An update. *Retrovirology* 10, 67 (**2013**).
8. L. Redel, V. Le Douce, T. Cherrier, C. Marban, A. Janossy, D. Aunis, C. Van Lint, O. Rohr, and C. Schwartz, HIV-1 regulation of latency in the monocyte-macrophage lineage and in $CD4^+$ T lymphocytes. *J. Leukoc. Biol.* 87, 575 (**2010**).
9. K. Barton, B. Hiener, A. Winckelmann, T. A. Rasmussen, W. Shao, K. Byth, R. Lanfear, A. Solomon, J. McMahon, S. Harrington, M. Buzon, M. Lichterfeld, P. W. Denton, R. Olesen, L. Ostergaard, M. Tolstrup, S. R. Lewin, O. S. Sogaard, and S. Palmer, Broad activation of latent HIV-1 *in vivo*. *Nat. Commun.* 7, 12731 (**2016**).
10. H. Yang, S. Buisson, G. Bossi, Z. Wallace, G. Hancock, C. So, R. Ashfield, A. Vuidepot, T. Mahon, P. Molloy, J. Oates, S. J. Paston, M. Aleksic, N. J. Hassan, B. K. Jakobsen, and L. Dorrell, Elimination of latently HIV-infected cells from antiretroviral therapy-suppressed subjects by engineered immune-mobilizing T-cell receptors. *Mol. Ther.* 24, 1913 (**2016**).
11. S. M. Saayman, D. C. Lazar, T. A. Scott, J. R. Hart, M. Takahashi, J. C. Burnett, V. Planelles, K. V. Morris, and M. S. Weinberg, Potent and targeted activation of latent HIV-1 using the CRISPR/dCas9 activator complex. *Mol. Ther.* 24, 488 (**2016**).
12. K. Ververis, A. Hiong, T. C. Karagiannis, and P. V. Licciardi, Histone deacetylase inhibitors (HDACIs): Multitargeted anticancer agents. *Biologics* 7, 47 (**2013**).
13. R. C. Desrosiers, D. G. Wei, V. Chiang, E. Fyne, M. Balakrishnan, T. Barnes, M. Graupe, J. Hesselgesser, A. Irrinki, J. P. Murry, G. Stepan, K. M. Stray, A. Tsai, H. Yu, J. Spindler, M. Kearney, C. A. Spina, D. McMahon, J. Lalezari, D. Sloan, J. Mellors, R. Geleziunas, and T. Cihlar, Histone deacetylase inhibitor romidepsin induces HIV expression in CD4 T cells from patients on suppressive antiretroviral therapy at concentrations achieved by clinical dosing. *PLoS Pathogens* 10, e1004071 (**2014**).
14. S. Bouchat, J. S. Gatot, K. Kabeya, C. Cardona, L. Colin, G. Herbein, S. De Wit, N. Clumeck, O. Lambotte, C. Rouzioux, O. Rohr, and C. Van Lint, Histone methyltransferase inhibitors induce HIV-1 recovery in resting CD4(+) T cells from HIV-1-infected HAART-treated patients. *AIDS* 26, 1473 (**2012**).
15. S. Y. Park, K. C. Kim, K. J. Hong, S. S. Kim, and B. S. Choi, Histone deactylase inhibitor SAHA induces a synergistic HIV-1 reactivation by 12-O-tetradecanoylphorbol-13-acetate in latently infected cells. *Intervirology* 56, 242 (**2013**).
16. H. Yin, Y. Zhang, X. Zhou, and H. Zhu, Histonedeacetylase inhibitor oxamflatin increase HIV-1 transcription by inducing histone modification in latently infected cells. *Mol. Biol. Rep.* 38, 5071 (**2011**).
17. F. Wightman, H. K. Lu, A. E. Solomon, S. Saleh, A. N. Harman, A. L. Cunningham, L. Gray, M. Churchill, P. U. Cameron, A. E. Dear, and S. R. Lewin, Entinostat is a histone deacetylase inhibitor selective for class 1 histone deacetylases and activates HIV production from latently infected primary T cells. *AIDS* 27, 2853 (**2013**).
18. A. F. Victoriano, K. Imai, H. Togami, T. Ueno, K. Asamitsu, T. Suzuki, N. Miyata, K. Ochiai, and T. Okamoto, Novel histone

deacetylase inhibitor NCH-51 activates latent HIV-1 gene expression. *FEBS Lett.* 585, 1103 **(2011)**.

19. Y. Kobayashi, C. Gelinas, and J. P. Dougherty, Histone deacetylase inhibitors containing a benzamide functional group and a pyridyl cap are preferentially effective human immunodeficiency virus-1 latency-reversing agents in primary resting $CD4^+$ T cells. *J. Gen. Virol.* 98, 799 **(2017)**.

20. N. M. Archin, A. L. Liberty, A. D. Kashuba, S. K. Choudhary, J. D. Kuruc, A. M. Crooks, D. C. Parker, E. M. Anderson, M. F. Kearney, M. C. Strain, D. D. Richman, M. G. Hudgens, R. J. Bosch, J. M. Coffin, J. J. Eron, D. J. Hazuda, and D. M. Margolis, Administration of vorinostat disrupts HIV-1 latency in patients on antiretroviral therapy. *Nature* 487, 482 **(2012)**.

21. O. S. Sogaard, M. E. Graversen, S. Leth, R. Olesen, C. R. Brinkmann, S. K. Nissen, A. S. Kjaer, M. H. Schleimann, P. W. Denton, W. J. Hey-Cunningham, K. K. Koelsch, G. Pantaleo, K. Krogsgaard, M. Sommerfelt, R. Fromentin, N. Chomont, T. A. Rasmussen, L. Ostergaard, and M. Tolstrup, The depsipeptide romidepsin reverses HIV-1 latency *in vivo*. *PLoS Pathog.* 11, e1005142 **(2015)**.

22. M. E. Manson McManamy, S. Hakre, E. M. Verdin, and D. M. Margolis, Therapy for latent HIV-1 infection: The role of histone deacetylase inhibitors. *Antivir. Chem. Chemother.* 23, 145 **(2014)**.

23. T. A. Rasmussen, O. S. Sogaard, C. Brinkmann, F. Wightman, S. R. Lewin, J. Melchjorsen, C. Dinarello, L. Ostergaard, and M. Tolstrup, Comparison of HDAC inhibitors in clinical development: Effect on HIV production in latently infected cells and T-cell activation. *Hum. Vaccin. Immunother.* 9, 993 **(2013)**.

24. D. G. Wei, V. Chiang, E. Fyne, M. Balakrishnan, T. Barnes, M. Graupe, J. Hesselgesser, A. Irrinki, J. P. Murry, G. Stepan, K. M. Stray, A. Tsai, H. Yu, J. Spindler, M. Kearney, C. A. Spina, D. McMahon, J. Lalezari, D. Sloan, J. Mellors, R. Geleziunas, and T. Cihlar, Histone deacetylase inhibitor romidepsin induces HIV expression in CD4 T cells from patients on suppressive antiretroviral therapy at concentrations achieved by clinical dosing. *PLoS Pathog.* 10, e1004071 **(2014)**.

25. A. M. Spivak, A. Bosque, A. H. Balch, D. Smyth, L. Martins, and V. Planelles, *Ex vivo* bioactivity and HIV-1 latency reversal by ingenol dibenzoate and panobinostat in resting CD4(+) T cells from aviremic patients. *Antimicrob. Agents Chemother.* 59, 5984 **(2015)**.

26. W. G. Singleton, A. M. Collins, A. S. Bienemann, C. L. Killick-Cole, H. R. Haynes, D. J. Asby, C. P. Butts, M. J. Wyatt, N. U. Barua, and S. S. Gill, Convection enhanced delivery of panobinostat (LBH589)-loaded pluronic nano-micelles prolongs survival in the F98 rat glioma model. *Int. J. Nanomedicine* 12, 1385 **(2017)**.

27. P. Tsai, G. Wu, C. E. Baker, W. O. Thayer, R. A. Spagnuolo, R. Sanchez, S. Barrett, B. Howell, D. Margolis, D. J. Hazuda, N. M. Archin, and J. V. Garcia, *In vivo* analysis of the effect of panobinostat on cell-associated HIV RNA and DNA levels and latent HIV infection. *Retrovirology* 13, 36 **(2016)**.

28. T. A. Rasmussen, M. Tolstrup, C. R. Brinkmann, R. Olesen, C. Erikstrup, A. Solomon, A. Winckelmann, S. Palmer, C. Dinarello, M. Buzon, M. Lichterfeld, S. R. Lewin, L. Ostergaard, and O. S. Sogaard, Panobinostat, a histone deacetylase inhibitor, for latent-virus reactivation in HIV-infected patients on suppressive antiretroviral therapy: A phase 1/2, single group, clinical trial. *Lancet HIV* 1, e13 **(2014)**.

29. H. Wang, Z. Feng, and B. Xu, Bioinspired assembly of small molecules in cell milieu. *Chem. Soc. Rev.* 46, 2421 **(2017)**.

30. X. Du, J. Zhou, J. Shi, and B. Xu, Supramolecular hydrogelators and hydrogels: From soft matter to molecular biomaterials. *Chem. Rev.* 115, 13165 **(2015)**.

31. Z. Luo, Q. Wu, C. Yang, H. Wang, T. He, Y. Wang, Z. Wang, H. Chen, X. Li, C. Gong, and Z. Yang, A powerful CD8(+) T-cell stimulating D-tetra-peptide hydrogel as a very promising vaccine adjuvant. *Adv. Mater.* 29, 1601776 **(2017)**.

32. J. Shi, P. W. Kantoff, R. Wooster, and O. C. Farokhzad, Cancer nanomedicine: Progress, challenges and opportunities. *Nat. Rev. Cancer* 17, 20 **(2017)**.

33. S. Su, Y. Tian, Y. Li, Y. Ding, T. Ji, M. Wu, Y. Wu, and G. Nie, "Triple-punch" strategy for triple negative breast cancer therapy with minimized drug dosage and improved antitumor efficacy. *ACS Nano* 9, 1367 **(2015)**.

34. Y. Zhang, J. Wei, J. Xu, W. S. Leong, G. Liu, T. Ji, Z. Cheng, J. Wang, J. Lang, Y. Zhao, L. You, X. Zhao, T. Wei, G. J. Anderson, S. Qi, J. Kong, G. Nie, and S. Li, Suppression of tumor energy supply by liposomal nanoparticle-mediated inhibition of aerobic glycolysis. *ACS Appl. Mater. Interfaces* 10, 2347 **(2018)**.

35. Y. Qi, H. Min, A. Mujeeb, Y. Zhang, X. Han, X. Zhao, G. J. Anderson, Y. Zhao, and G. Nie, Injectable hexapeptide hydrogel for localized chemotherapy prevents breast cancer recurrence. *ACS Appl. Mater. Interfaces* 10, 6972 **(2018)**.

36. A. Jordan, D. Bisgrove, and E. Verdin, HIV reproducibly establishes a latent infection after acute infection of T cells *in vitro*. *Embo J.* 22, 1868 **(2003)**.

37. K. Melikov, A. Hara, K. Yamoah, E. Zaitseva, E. Zaitsev, and L. V. Chernomordik, Efficient entry of cell-penetrating peptide nonaarginine into adherent cells involves a transient increase in intracellular calcium. *Biochem. J.* 471, 221 **(2015)**.

38. R. Brock, The uptake of arginine-rich cell-penetrating peptides: Putting the puzzle together. *Bioconjug. Chem.* 25, 863 **(2014)**.

39. T. Ji, Y. Ding, Y. Zhao, J. Wang, H. Qin, X. Liu, J. Lang, R. Zhao, Y. Zhang, J. Shi, N. Tao, Z. Qin, and G. Nie, Peptide assembly integration of fibroblast-targeting and cell-penetration features for enhanced antitumor drug delivery. *Adv. Mater.* 27, 1865 **(2015)**.

40. S. T. Yang, A. J. B. Kreutzberger, J. Lee, V. Kiessling, and L. K. Tamm, The role of cholesterol in membrane fusion. *Chem. Phys. Lipids* 199, 136 **(2016)**.

41. D. Papahadjopoulos, M. Cowden, and H. Kimelberg, Role of cholesterol in membranes. Effects on phospholipid-protein interactions, membrane permeability and enzymatic activity. *Biochim. Biophys. Acta* 330, 8 **(1973)**.

42. J. Kroes and R. Ostwald, Erythrocyte membranes-effect of increased cholesterol content on permeability. *Biochim. Biophys. Acta* 249, 647 **(1971)**.

43. G. Chen-Yu, Y. Chun-Fen, L. Qi-Lu, T. Qi, X. Yan-Wei, L. Wei-Na, and Z. Guang-Xi, Development of a quercetin-loaded nanostructured lipid carrier formulation for topical delivery. *Int. J. Pharm.* 430, 292 **(2012)**.

44. G. Clutton, Y. Xu, P. L. Baldoni, K. R. Mollan, J. Kirchherr, W. Newhard, K. Cox, J. D. Kuruc, A. Kashuba, R. Barnard, N. Archin, C. L. Gay, M. G. Hudgens, D. M. Margolis, and N. Goonetilleke, The differential short- and long-term effects of HIV-1 latency-reversing agents on T cell function. *Scientific Reports* 6, 30749 **(2016)**.

45. C. Van Lint, S. Emiliani, M. Ott, and E. Verdin, Transcriptional activation and chromatin remodeling of the HIV-1 promoter in response to histone acetylation. *EMBO J.* 15, 1112 **(1996)**.

46. S. Hakre, L. Chavez, K. Shirakawa, and E. Verdin, Epigenetic regulation of HIV latency. *Curr. Opin. HIV AIDS* 6, 19 **(2011)**.

47. N. M. Archin, A. Espeseth, D. Parker, M. Cheema, D. Hazuda, and D. M. Margolis, Expression of latent HIV induced by the potent HDAC inhibitor suberoylanilide hydroxamic acid. *AIDS Res. Hum. Retroviruses* 25, 207 **(2009)**.